From Pixels to Diagnosis: An Innovative EfficientNetB3 Approach for Interpreting Lung and Colon Cancer Histopathology

***Abstract*—Globally, lung and colon cancers are predominant contributors to cancer mortality.. Early and accurate diagnosis is crucial for effective treatment. While deep learning models have shown promise in automating cancer classification from histopathological images, challenges remain in achieving high accuracy while maintaining interpretability. This research focuses on creating a high-efficiency and interpretable deep learning model for identifying lung and colon cancer from histopathological images. We propose a novel approach based on a modified EfficientNetB3 architecture. The model was trained on a dataset of 25,000 high-resolution histopathological images across five classes. We integrated Explainable AI (XAI) techniques, specifically LIME and SHAP, to enhance model interpretability. Our proposed model achieved an exceptional accuracy of 99.66%, outperforming other state-of-the-art architectures. The model demonstrated high precision (99.78%), recall (98.58%), and F1-score (99.18%). The incorporation of LIME and SHAP offered significant understanding into how the model makes decisions, emphasizing relevant histological characteristics that affect classification. This study presents a highly accurate and interpretable deep learning model for lung and colon cancer classification. The combination of superior performance and explainability addresses a critical need in medical AI applications.**

***Index Terms*—Lung and Colon Cancer Classification, Deep Learning, Histopathological Image Analysis, EfficientNetB3, Explainable AI**

I. Introduction

With millions of new cases reported annually, lung and colon cancer are among the most common and fatal malignancies known to exist worldwide. Effective therapy and better patient outcomes depend on early, correct diagnosis [1]. Conventional approaches of identifying these tumors, such biopsy and histological analysis, are time-consuming and mostly dependent on the knowledge of pathologists, so there is possible variation in diagnosis. Advances in artificial intelligence (AI) [2], especially in the domain of deep learning, have shown considerable potential in automating the classification of malignant tissues from medical images, hence supporting faster and more consistent diagnosis.

As deep learning models—especially convolutional neural networks (CNNs) [3]–[5] can automatically learn and extract hierarchical features from raw images—they have been extensively explored for image classification tasks. These include the need for large labeled datasets, high computational [6] resources, and the necessity for models that are both accurate and interpretable by clinicians.

This work suggests a novel method based on a modified EfficientNetB3 model improved with Explainable AI (XAI) approaches to the categorisation of lung and colon cancer. This work intends to build a model that not only achieves great accuracy but also gives interpretable findings that can be accepted by medical professionals by combining lightweight and efficient neural network designs with robust feature extracting and attention techniques. Using XAI methods include LIME (Local Interpretable Model-agnostic Explanations) and SHAP (SHapley Additive exPlanations) guarantees that the model's decision-making process is open, therefore eliminating one of the main obstacles to the acceptance of AI in clinical practice [7].

The major contributions of this study are:

1) The proposed EfficientNetB3 model achieved superior performance in lung and colon cancer classification, with an accuracy of 99.66%, outperforming other state-of-the-art architectures.
2) The research incorporated LIME and SHAP to enhance model interpretability, addressing a critical need in medical AI applications.
3) By achieving high accuracy and providing interpretability, the proposed model shows potential for enhancing precision in clinical diagnostics for lung and colon cancer.

Building on current developments in artificial intelligence and medical imaging, this work seeks to support the continuous efforts to enhance cancer detection and treatment using technology, hence producing better patient outcomes [8].

The remainder of this paper is structured as follows: Section II reviews relevant literature on lung and colon cancer classification using deep learning. Section III details our methodology, including dataset preparation, model architectures, and evaluation metrics. Section IV presents and analyzes our results, comparing various models with a focus on our proposed EfficientNetB3 architecture. Section V introduces the Explainable AI techniques (LIME and SHAP) used to interpret our model. Section VI discusses our findings in the context of recent research and potential clinical applications. Finally, Section VII concludes the paper, summarizing key contributions and suggesting future research directions.

II. Literature Review

The classification of lung and colon cancers using histopathology images has been significantly enhanced by deep learning. To increase the efficiency and capability of the

models various methods have been handcrafted to face the challenge that comes with medical diagnosis.

A. Deep Learning Models for Cancer Classification

Among the available studies,some have concentrated on utilising CNNs to classify lung and colon cancer. The authors of [3] employed a pre-trained VGG19 model that demonstrated good accuracy.But this comes at the cost of high model complexity and computation capability which hinders real life applications. In contrast, the authors of [9] proposed DNN models that show exceptional results on various datasets,containing both histopathology and CT pictures.

B. Feature Engineering and Hybrid Systems

Although deep learning models have become popular, the combination of feature engineering with standard machine learning models continues to be beneficial. This is demonstrated by the authors of [10], who achieved good interpretability and accuracy by using XGBoost. The authors of Paper [11] improved performance by integrating Convolutional Neural Network (CNN) with manually designed features, resulting in an accuracy of 99.64%. This goes to show the effectiveness of mixing both advanced and basic features that were extracted.

C. Explainability and Interpretability in AI Models

For AI models to be used and familiarized in clinical practice, they need to be made explainable. Similar work done in [2], [12], [13], have incorporated explainable AI (XAI) techniques, including Grad-Cam ,LIME and SHAP. In clinical practice, these methods enhance transparency and trust in AI-driven decisions by providing visual and interpret-able explanations for model predictions.

D. Comparative Analysis of Model Architectures

In these investigations, numerous Convolutional Neural Network (CNN) designs, including VGG19, DenseNet, ResNet, and EfficientNet, have been examined. Each architecture offers unique benefits regarding precision, computational performance, and appropriateness for particular medical imaging applications. As an illustration, the authors of [2] introduced a streamlined multi-scale CNN model that attained exceptional precision while minimising intricacy. This characteristic renders it well-suited for real-time applications.

Similarly, [12] shows the capability of EfficientNetV2 models in terms of high-accuracy classification with XAI features. This goes to show the trend towards efficient and interpretable AI models.

Adding the Global Context (GC) attention module in [13] shows a notable progress in improving model efficiency while minimising computing expenses. This innovation enhances the accuracy of classification while simultaneously decreasing the number of parameters and the time it takes for the model to make inferences. As a result, it is well-suited for use on mobile devices. The study's simultaneous emphasis on accuracy at both the image-level and patient-level exemplifies a complete approach to cancer categorisation.

Currently in biomedical image processing, specially in AI-driven cancer detection there is a trend towards developing models that boast balanced accuracy, efficiency, and interpretability. The integration of feature engineering, hybrid systems, and XAI techniques presents a promising direction for improving the reliability and transparency of AI models in clinical settings. The proposed work in this study, particularly the use of a tailored EfficientNetB3 model combined with XAI techniques, aligns well with these trends, offering a robust solution for lung and colon cancer classification using histopathology images.

III. Methodology

"Fig. 1" demonstrates the methodological flow of the study.

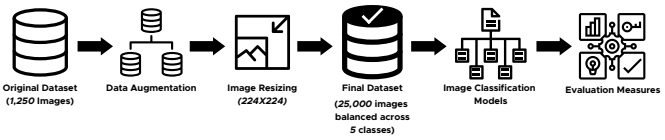

Fig. 1: Methodology Diagram

A. Dataset and Pre-processing

The study utilized a dataset [14] of 25,000 high-resolution histopathological images (768 $\times$ 768 pixels, JPEG format) across five classes. The dataset originated from 1,250 HIPAA-compliant images, comprising 750 lung tissue images (250 each of benign, adenocarcinoma, and squamous cell carcinoma) and 500 colon tissue images (250 each of benign and adenocarcinoma). Using the `Augmentor` package, the original set was expanded to 25,000 images. We resized the images to 224 $\times$ 224 pixels. This augmentation process resulted in a balanced distribution across five classes, each containing 5,000 images. The augmentation enhanced dataset robustness while preserving original tissue characteristics, providing a comprehensive foundation for machine learning models in histopathological image analysis, particularly for lung and colon cancer detection and classification.

B. Image Classification Models

1) EfficientNetB3: Compound scaling is used by EfficientNetB3 to achieve network width, depth, and resolution balance. It has integrated squeeze-and-excitation modules and MBConv blocks. The model employs Swish activation functions and a compound scaling factor to optimize efficiency and accuracy.

2) Xception: Xception extends the Inception model with three main flows: entry, middle, and exit. The model employs depth-wise separable convolutions instead of the Inception modules. Additionally, the architecture integrates residual connections to assist gradient flow during training, thereby improving performance while retaining computational efficiency.

3) InceptionV3: Asymmetric convolutions, factorized convolutions, and auxiliary classifiers are aspects of InceptionV3. It makes use of max-pooling and parallel strided convolution for effective grid size reduction. These innovations allow high accuracy with minimized computational cost.

4) ResNet50: ResNet50 is built on residual learning, with four stages of residual blocks containing bottleneck units. It uses skip connections to mitigate the vanishing gradient problem, enabling the training of very deep networks. The architecture begins with initial convolution and ends with global average pooling and a fully connected layer.

5) VGG16: VGG16 has a uniform, deep structure with five blocks of convolutional layers (3×3 filters) followed by max pooling. It features three fully connected layers, with the channel depths being doubled following each max pooling layer. The straightforward yet deep architecture makes it highly effective for a wide range of computer vision applications.

6) Basic CNN: The basic CNN comprises five convolutional blocks, a flattening layer, three dense blocks, and an output layer. Convolutional blocks increase in filter count (16 to 256), while dense blocks decrease in size (128 to 32 units) with dropout for regularization. The model ends with a sigmoid-activated output layer for multi-label classification.

C. Proposed Model

The model proposed is an adaptation of the EfficientNetB3 to a refined version for distinguishing lung and colon cancer. This architecture combines the strong feature extraction capabilities of EfficientNetB3 with some new custom layers to improve performance. "Fig. 2" depicts the architecture of the proposed model.

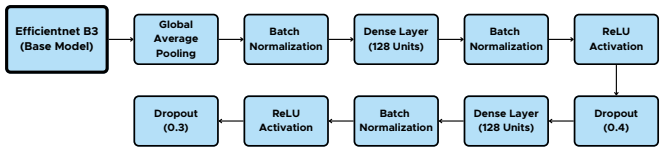

Fig. 2: Proposed EfficientNetB3 Model Architecture

Building upon this robust foundation, we introduce several custom layers to fine-tune the network:

1) **Global Average Pooling:** Following the base model, we incorporate a Global Average Pooling layer. This layer reduces the spatial dimensions of the feature maps, effectively minimizing the number of parameters and mitigating potential overfitting.
2) **Fully Connected Layers:** We introduce two dense layers in a descending structure to progressively refine the extracted features:
   a) The first dense layer consists of 128 units, allowing for rich feature representation.
   b) The second dense layer further reduces dimensionality to 64 units, distilling the most salient features for classification.
3) **Batch Normalization:** Batch normalization is applied after each dense layer. By standardizing activations, this technique enhances the stability of the neural network during training and facilitates greater generalization.
4) **Activation Function:** We use the ReLU activation function after every layer of dense data. ReLU adds non-linearity to the model, allowing it to discover intricate links and patterns in the data.
5) **Dropout Regularization:** To mitigate overfitting and enhance the model's generalization performance, dropout layers are included:
   a) A dropout rate of 40% is applied after the first dense layer.
   b) A reduced dropout rate of 30% follows the second dense layer.

   This progressive reduction in dropout rate aligns with the narrowing structure of our network.
6) **Output Layer:** The last part of the model architecture is a fully connected layer with neurons that match the number of categories in the classification task. This layer employs a sigmoid activation function, producing probability distributions for each class.

D. Evaluation Measures

We evaluated the performance of our algorithm to classify lung and colon cancers based on various evaluation metrics. These metrics cover a broad overview of cancer types and normal tissues distinction ability for an algorithm.

1) Accuracy: The primary metric employed was accuracy, which indicates how accurate all of the model's outputs are:

$$\text{Accuracy} = \frac{\text{Number of correct predictions}}{\text{Total number of predictions}} \tag{1}$$

This measure provides a high-level summary of all classes' performance for the model.

2) Precision: Calculated for each class, precision evaluates the model's capacity to prevent false positives:

$$\text{Precision} = \frac{\text{True Positives}}{\text{True Positives} + \text{False Positives}} \tag{2}$$

High precision indicates that when the model predicts a specific cancer type, it is likely to be correct.

3) Recall: Recall, also known as sensitivity, evaluates the model's capacity to identify all positive instances:

$$\text{Recall} = \frac{\text{True Positives}}{\text{True Positives} + \text{False Negatives}} \tag{3}$$

A high recall indicates that all cases of a specific cancer type may be detected by the model.

4) F1-Score: The F1-score provides a balanced measure of precision and recall:

$$\text{F1-Score} = 2 \times \frac{\text{Precision} \times \text{Recall}}{\text{Precision} + \text{Recall}} \tag{4}$$

IV. Result Analysis

In our study, we employed a dataset split of 70% for training, 10% for validation, and 10% for testing. This distribution ensured a robust training process while reserving sufficient data for model validation and final performance evaluation. The experiments were conducted in a high-performance computing environment using Google Colab with an A100 GPU, allowing for efficient model training and evaluation over 10 epochs.

TABLE I: Performance Comparison of Different Models

Model	Accuracy	Precision	Recall	F1-Score
Xception	95.60%	94.70%	95.70%	95.20%
Inception	93.80%	92.90%	94.20%	93.54%
ResNet50	94.50%	93.80%	94.70%	94.25%
VGG16	92.70%	91.90%	93.10%	92.50%
CNN	91.20%	90.50%	91.60%	91.04%
EfficientNetB3	94.80%	94.20%	94.90%	94.55%
Proposed EfficientNetB3	**99.66%**	**99.78%**	**98.58%**	**99.18%**

Table I depicts the performance analysis of different deep learning models. Our proposed EfficientNetB3 model demonstrated superior performance compared to other state-of-the-art architectures in this classification task. Achieving an impressive accuracy of 99.66%, the EfficientNetB3 model surpassed the next best performer, Xception, by 4.06 percentage points. This significant improvement extends across all key performance metrics, with the EfficientNetB3 model showcasing exceptional precision (99.78%), recall (98.58%), and F1-score (99.18%). The outstanding results of the EfficientNetB3 model can be credited to various elements. The model's compound scaling method allows it to achieve a better balance between accuracy and computational efficiency compared to other models tested. "Fig. 3" and "Fig. 4" represents the performance curves of the proposed model throughout training.

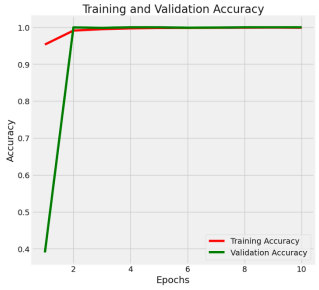

Fig. 3: Training and Validation Accuracy

Fig. 4: Training and Validation Loss

The confusion matrix "Fig. 5" demonstrates the EfficientNetB3 model's exceptional performance. It achieved perfect classification in four out of five classes, with only one misclassification between Lung Squamous Cell Carcinoma and Lung Adenocarcinoma. This near-perfect accuracy across various cancer types and tissue samples, including precise differentiation between benign and malignant tissues, underscores the model's potential for high-precision clinical diagnostics.

V. Explainable AI Techniques

To enhance model interpretability, we implemented LIME and SHAP.

A. LIME Analysis

LIME highlights image areas influencing classification decisions. "Fig. 6" shows a sample LIME explanation, where

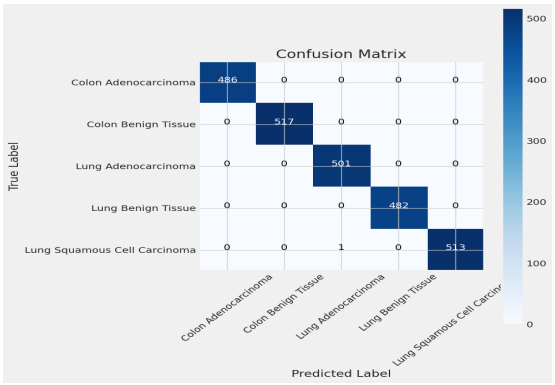

Fig. 5: Confusion Matrix of the EfficientNetB3 model's performance

yellow regions indicate areas supporting the model's classification.

Fig. 6: LIME explanation for a histopathological image. Left: Original image. Middle and Right: LIME outputs highlighting influential regions.

The visualization reveals the model's focus on specific cellular structures and patterns, aligning with known diagnostic criteria and suggesting the model has learned relevant features for cancer classification.

B. SHAP Analysis

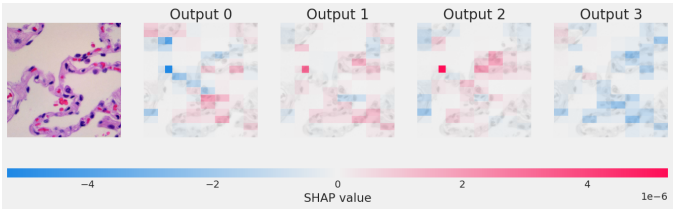

Fig. 7: SHAP analysis for a histopathological image. Left: Original image. Right: Four SHAP outputs showing feature importance.

SHAP determines feature importance using Shapley values. "Fig. 7" presents a SHAP analysis with four output visualizations.

VI. Discussion

Table II compares our proposed EfficientNetB3 model with other recent approaches in lung and colon cancer classification. Our model demonstrates superior performance, achieving the

TABLE II: Comparison of Lung and Colon Cancer Classification Models

Author	Model	XAI	Acc. (%)	Prec. (%)	Rec. (%)	F1 (%)
[15]	CNN	✗	96.33	96.39	96.37	96.38
[16]	CNN	✗	99.00	-	-	-
[17]	XGBoost	✓	95.60	95.80	96.00	95.90
[2]	LW-MS-CCN	✓	99.20	99.16	99.36	99.16
Ours	**Proposed EfficientNetB3**	✓	**99.66**	**99.78**	**98.58**	**99.18**

highest accuracy (99.66%) and precision (99.78%) among the compared methods. Notably, it outperforms the LW-MS-CCN model [2], which previously held the highest accuracy of 99.20%. A key advantage of our approach is the integration of Explainable AI (XAI) techniques, which is absent in some earlier high-performing models [15], [16]. This combination of superior accuracy and interpretability sets our model apart in the field of medical image analysis.

There are various reasons for the improved performance of our proposed EfficientNetB3 model. The EfficientNetB3 architecture's compound scaling method optimally balances network depth, width, and resolution, enabling more effective feature extraction from histopathological images. Additionally, our use of transfer learning, utilizing pre-trained weights on ImageNet, allows the model to leverage general image features [18], enhancing its ability to detect subtle patterns in medical images. Our custom top layers, global average pooling and strategically positioned dense layers with dropout help to further improve the model's performance and customize it for tasks related to cancer classification. In addition to offering insights into the decision-making process, the combination of LIME and SHAP for model interpretation aligns with the model's emphasis regions with clinically relevant features, potentially enhancing the model's acceptability and dependability in medical contexts. This interpretability, combined with the model's high accuracy, addresses a critical need in medical AI applications where understanding the basis of diagnoses is as important as the diagnoses themselves.

VII. Conclusion

This research introduces an innovative method for classifying lung and colon cancers through histopathological images, attaining a cutting-edge accuracy of 99.66%. Our proposed model, based on a modified EfficientNetB3 architecture, outperformed existing methods in terms of accuracy, precision, and F1-score. The integration of Explainable AI techniques, specifically LIME and SHAP, addresses a critical need in medical AI applications by providing interpretable insights into the model's decision-making process.

The novelty of our research lies in the successful combination of a highly efficient deep learning architecture with advanced interpretability methods. This approach not only achieves superior classification performance but also enhances the potential for clinical adoption by providing transparent, explainable results. Our model's ability to accurately distinguish between different cancer types and benign tissues, while highlighting relevant histological features, represents a significant advancement in automated cancer diagnosis.

Despite these achievements, limitations exist. The study was conducted on a specific dataset, and further validation on diverse, multi-institutional datasets is necessary to ensure generalizability. Additionally, while our model shows high accuracy, the interpretability of DL models in medical contexts remains an ongoing challenge.

Future work should focus on expanding the model's capabilities to include a broader range of cancer types and stages. Integration with clinical workflows and prospective studies in real-world settings will be crucial for validating the model's practical utility. Furthermore, exploring more advanced XAI techniques and their alignment with clinical expertise could further bridge the gap between AI-assisted diagnosis and clinical practice.

References

[1] G. Litjens, T. Kooi, B. E. Bejnordi, A. A. A. Setio, F. Ciompi, M. Ghafoorian, J. A. van der Laak, B. van Ginneken, and C. I. Sánchez, "A survey on deep learning in medical image analysis," *Medical image analysis*, vol. 42, pp. 60–88, 2017.

[2] M. A. Hasan, F. Haque, S. R. Sabuj, H. Sarker, M. O. F. Goni, F. Rahman, and M. M. Rashid, "An end-to-end lightweight multi-scale cnn for the classification of lung and colon cancer with xai integration," *Technologies*, vol. 12, no. 4, p. 56, 2024.

[3] B. L. Qasthari, E. Susanti, and M. Sholeh, "Classification of lung and colon cancer histopathological images using convolutional neural network (cnn) method on a pre-trained models," *International Journal of Applied Sciences and Smart Technologies*, vol. 5, no. 1, pp. 133–142, 2023.

[4] A. Esteva, B. Kuprel, R. A. Novoa, J. Ko, S. M. Swetter, H. M. Blau, and S. Thrun, "Dermatologist-level classification of skin cancer with deep neural networks," *Nature*, vol. 542, no. 7639, pp. 115–118, 2017.

[5] Z. Ahmed and S. S. Shanto, "Performance analysis of yolo architectures for surgical waste detection in post-covid-19 medical waste management," *Malaysian Journal of Science and Advanced Technology*, pp. 1–9, 2024.

[6] M. Bilal, S. E. A. Raza, A. Azam, S. Graham, M. Ilyas, and N. M. Rajpoot, "Development and validation of a weakly supervised deep learning framework to predict the status of molecular pathways and key mutations in colorectal cancer from routine histology images: a retrospective study," *The Lancet Digital Health*, vol. 3, no. 12, pp. e763–e772, 2021.

[7] U. Djuric, G. Zadeh, K. Aldape, and P. Diamandis, "Precision histology: how deep learning is poised to revitalize histomorphology for personalized cancer care," *NPJ precision oncology*, vol. 1, no. 1, pp. 1–6, 2017.

[8] S. Wang, L. Kong, B. Zhang, J. Dong, and Y. Li, "Classification of lung cancer subtype by tissue image analysis using convolutional neural network," *BioMed Research International*, vol. 2020, 2020.

[9] A. H. Uddin, Y.-L. Chen, M. R. Akter, C. S. Ku, J. Yang, and L. Y. Por, "Colon and lung cancer classification from multi-modal images using resilient and efficient neural network architectures," *Heliyon*, vol. 10, no. 9, 2024.

[10] A. Hage Chehade, N. Abdallah, J.-M. Marion, M. Oueidat, and P. Chauvet, "Lung and colon cancer classification using medical imaging: A feature engineering approach," *Physical and Engineering Sciences in Medicine*, vol. 45, no. 3, pp. 729–746, 2022.

[11] M. Al-Jabbar, M. Alshahrani, E. M. Senan, and I. A. Ahmed, "Histopathological analysis for detecting lung and colon cancer malignancies using hybrid systems with fused features," *Bioengineering*, vol. 10, no. 3, p. 383, 2023.

[12] S. Tummala, S. Kadry, A. Nadeem, H. T. Rauf, and N. Gul, "An explainable classification method based on complex scaling in histopathology images for lung and colon cancer," *Diagnostics*, vol. 13, no. 9, p. 1594, 2023.

[13] M. A.-M. Provath, K. Deb, P. K. Dhar, and T. Shimamura, "Classification of lung and colon cancer histopathological images using global context attention based convolutional neural network," *IEEE Access*, 2023.

[14] A. A. Borkowski, M. M. Bui, L. B. Thomas, C. P. Wilson, L. A. DeLand, and S. M. Mastorides, "Lung and colon cancer histopathological image dataset (lc25000)," *arXiv preprint arXiv:1912.12142*, 2019.

[15] M. Masud, N. Sikder, A.-A. Nahid, A. K. Bairagi, and M. A. AlZain, "A machine learning approach to diagnosing lung and colon cancer using a deep learning-based classification framework," *Sensors*, vol. 21, no. 3, p. 748, 2021.

[16] B. Ananthakrishnan, A. Shaik, S. Chakrabarti, V. Shukla, D. Paul, and M. S. Kavitha, "Smart diagnosis of adenocarcinoma using convolution neural networks and support vector machines," *Sustainability*, vol. 15, no. 2, p. 1399, 2023.

[17] A. Hage Chehade, N. Abdallah, J.-M. Marion, M. Oueidat, and P. Chauvet, "Lung and colon cancer classification using medical imaging: A feature engineering approach," *Physical and Engineering Sciences in Medicine*, vol. 45, no. 3, pp. 729–746, 2022.

[18] K. Sirinukunwattana, S. E. A. Raza, Y. W. Tsang, D. R. Snead, I. A. Cree, and N. M. Rajpoot, "Locality sensitive deep learning for detection and classification of nuclei in routine colon cancer histology images," *IEEE Transactions on Medical Imaging*, vol. 35, no. 5, pp. 1196–1206, 2016.